Journal of the Geological Society, London, Vol. **150**, 1993, pp. 393–404, 15 figs, 2 tables Printed in Northern Ireland

Tectonic evolution of the Nakasib suture, Red Sea Hills, Sudan: evidence for a late Precambrian Wilson Cycle

M. G. ABDELSALAM & R. J. STERN
The University of Texas at Dallas, Programs in Geosciences, PO Box 830688, Richardson, Texas, 75083-0688, USA

Abstract: The Nakasib suture is a late Proterozoic (Pan-African) ophiolite-decorated structural belt in the central Red Sea Hills of the Sudan. It represents one of the sutures along which the island arc/back-arc terranes and continental microplates of the Arabian–Nubian Shield are welded together. The Nakasib suture separates the 900–850 Ma old Haya terrane in the south from the 830–720 Ma old Gebeit terrane to the north. Five thrust-bounded stratigraphical groups are identified across the suture. These are, from south to north, Arbaat volcanic group (*c*. 730 Ma rift-related volcanic rocks), Salatib group (early passive margin volcanic and sedimentary rocks), Meritri group (the lower part of which contains alluvial and submarine fans of an incipient ocean basin, while its upper part can be tentatively equated with a platform of clastic sedimentary and carbonate intercalations which mark the stage of mature ocean basin opening), Nakasib ophiolite, and Shalhout group (arc-related volcanic and sedimentary rocks). These are intruded by syn-tectonic and post-tectonic plutonic rocks.

The tectonic setting of the above lithological groups suggests that the early stage of the Nakasib suture development was marked by rifting of older crust, probably the Haya terrane, which culminated in development of a passive margin on the south margin of an oceanic basin prior to collapse into an ophiolite-decorated suture. This indicates that the Nakasib suture evolved through a complete Wilson cycle orogeny from rifting, through passive margin formation, to closure of the basin and suturing.

The Arabian–Nubian Shield of NE Africa (Fig. 1) is an example of a late Proterozoic orogenic belt that formed by Phanerozoic-type plate tectonic processes (Kroner 1984). Geological work on the Shield emerges in two end-member tectonic models. (1) Accretion of intra-oceanic island arc and back-arc basin complexes (Almond 1982; Vail 1983, 1985; Embleton *et al.* 1984) and continental micro-plates (Camp 1984; Stoeser & Camp 1985; Kroner *et al.* 1987). These terranes are welded together along ophiolite-decorated sutures (Kroner 1985). Suture, in the context of this paper, does not imply the closure of a continent-separating ocean, but is applied to the closure of any basin floored by oceanic crust, where the accreted fragments may be a micro-continent, island arc, etc. This juvenile crust was accreted against the Nile craton to the west (Fig. 1; Abdelsalam & Dawoud 1991). (2) Opening and closing of short-lived oceanic basins. This is supported by the presence of ophiolite belts in the interior of what is suggested to be the Nile craton (Abdel Rahman *et al.* 1990) and the rift-related nature of some of the volcanic rocks of the Eastern Desert of Egypt (Stern *et al.* 1991).

This work on the Nakasib suture documents, for the first time, a complete Wilson cycle orogeny for a suture in the Arabian–Nubian Shield. Elements of this cycle include identification of *c*. 730 Ma old rift-related tholeiitic volcanic rocks, a passive margin sedimentary package, and a folded ophiolitic nappe that decorates the entire length of the Nakasib suture. A model between the above end-member models can best explain the tectonic evolution of this suture.

Regional setting of the Nakasib suture

The presence of ophiolite fragments along the Nakasib suture was first noted by Embleton *et al.* (1984) in the NE part of the belt (Fig. 2) whilst Kroner *et al.* (1987) identified another ophiolite complex occupying Jebel Tohado (Fig. 2). Almond & Ahmed (1987) reported another ophiolite occurrence at Jebel Igariri (Fig. 2). These ophiolite fragments define a NE-trending belt extending from north of Port Sudan in the NE to the Ariab area in the SW. There is general acceptance that this belt represents a suture separating two terranes (e.g. Vail 1983, 1985; Embleton *et al.* 1984; Kroner *et al.* 1987; Almond & Ahmed 1987; Almond *et al.* 1989). The terrane to the north was named the Gebeit terrane and that to the south the Haya terrane by Kroner *et al.* (1987). The Nakasib suture is offset by the younger, N- to NNW-trending Oko shear zone (Fig. 2). This offset is estimated to be about 30 km in a sinistral sense (Almond & Ahmed 1987). The Nakasib suture is thought to continue into Arabia as the Bir Umq suture (Vail 1983, 1985; Embleton *et al.* 1984; Camp 1984; Stoeser & Camp 1985; Kroner *et al.* 1987; Almond & Ahmed 1987; Pallister *et al.* 1988; Almond *et al.* 1989).

Almond & Ahmed (1987) suggested that the Nakasib suture evolved in two main stages. The first stage was subduction-related and caused ophiolite emplacement along an oceanic suture. The second stage was collision-related and resulted in shearing of the ophiolites within broad mylonite bands.

The region to the south of the Nakasib suture is occupied by the Haya terrane (Fig. 1). This NE-trending volcano-sedimentary belt includes arc-related volcanic rocks (Kroner *et al.* 1987). The central part of the Haya terrane is occupied by intensely folded high-grade rocks which include paragneisses and quartzites (I. M. Shaddad, pers. comm., 1990). The above assemblage was intruded by syn-tectonic granitoids of arc affinity (Klemenic & Poole 1988). Kroner *et al.* (1991) obtained U/Pb zircon ages of 830–870 Ma from several plutons in the Haya terrane. This led Kroner *et al.*

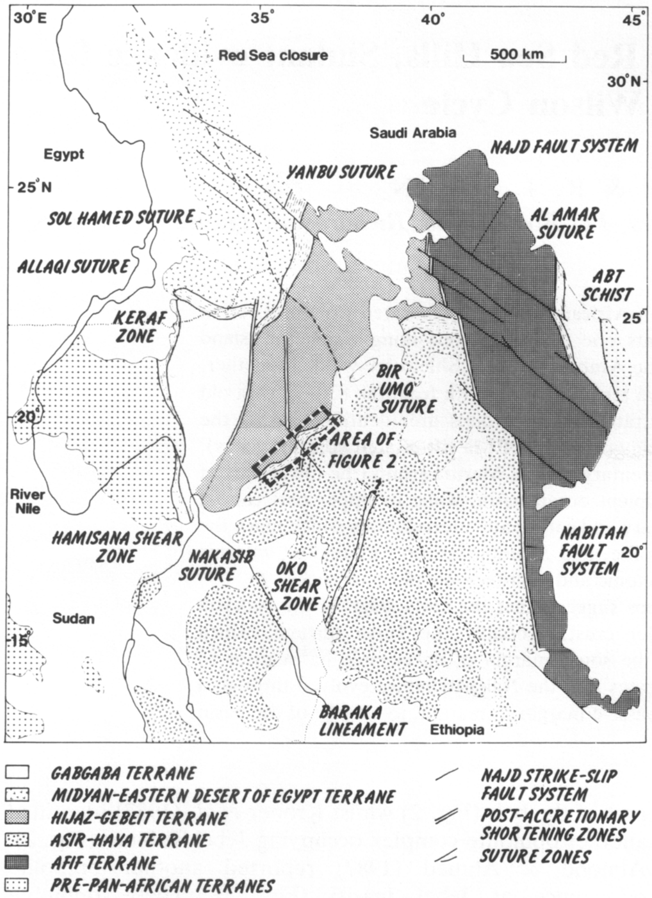

Fig. 1. Sketch geological map of the Arabian–Nubian Shield with Tertiary opening (dashed line) of the Red Sea restored (modified after Vail 1985).

(1991) to suggest that the Haya terrane is the extension of the 900–850 Ma old Asir terrane of Arabia (Fig. 1).

The Gebeit terrane comprises arc-related low-grade volcano-sedimentary sequences and syn-tectonic igneous complexes which occupy the area to the north of the Nakasib suture (Vail *et al.* 1984; Klemenic 1985; Klemenic *et al.* 1985). Whole rock Rb/Sr isochron ages around 720 Ma have been reported for volcanic and plutonic rocks from the terrane (Fitches *et al.* 1983; Klemenic 1985; Reischmann 1986; Klemenic & Poole 1988; Almond *et al.* 1989). However, older ages of about 830 Ma were obtained for other volcanic rocks using Sm-Nd dating methods (Reischmann 1986). This led Kroner *et al.* (1987) to suggest that the Gebeit terrane constitutes part of the 700–850 Ma old Hijaz terrane (Stoeser & Camp 1985).

Almond *et al.* (1989) attempted to bracket the age of deformation along the Nakasib suture. They obtained a whole rock Rb-Sr isochron age of 6971 ± 15 Ma for a syn-tectonic granite in the SW part of the suture (the Shalhout granite), and 552 ± 18 Ma for post-tectonic granite in the NE part (the Arbaat granite; Fig. 2). They concluded that the Nakasib suture formed prior to 700 Ma ago which is in general agreement with the time of arc accretion for the Arabian–Nubian Shield.

Stratigraphy of the Nakasib suture zone

The Nakasib suture is defined by NE-trending beds of sedimentary and volcanic rocks, some of which can be traced along the entire length of the suture. The original lithologies and primary structures of these rocks are generally well preserved in spite of a pervasive low-grade greenschist facies metamorphism. The stratigraphical divisions presented below are based on four main traverses along Khors Arbaat, Meritri, Youdib and across the western extension of the Nakasib suture west of the Oko shear zone (Fig. 2). Other short traverses include Khors Hasheit, Adenaiab, Yas, Samadi, Salatib, Tendily and Igariri (Fig. 2).

Our work indicates that the stratigraphy of the Nakasib suture can be divided into five groups and a suite of intrusive rocks (Figs 2 and 3). The five groups, the focus of this paper, are separated by thrusts. The group names are new. This stratigraphy is informal because structural complications make it impossible to know the original relations between units preserved in the nappes. Only the Arbaat volcanic group is believed to be autochthonous and is the northern margin of the Haya terrane. Thrust contacts separating these groups are sometimes very steep, due to folding by younger NE-trending, upright and horizontal folds (Abdelsalam & Stern, in prep.; Fig. 2).

Aye *et al.* (1987) divided the rocks along the Nakasib suture into three broad assemblages. (1) The Onib–Oshib ultramafic complex, which comprises the ophiolite belts of the Nakasib suture. (2) The Ariab series, which comprises volcanic and sedimentary rocks, and corresponds to our Salatib, Meritri and Shalhout groups. (3) The Awat series, which includes post-tectonic volcanic rocks. Our work indicates that this series is part of the Arbaat volcanic group as will be discussed below.

In the following sections we describe the major lithostratigraphic components of the Nakasib suture beginning with the Arbaat volcanic group and progressing north and generally up section.

The Arbaat volcanic group

This group is predominantly composed of mafic metavolcanic rocks with subordinate felsic metavolcanic rocks and minor sandstone and limestone beds and reaches a minimum thickness of about 2 km along Khor Salatib (Fig. 2). The base of the group has not been found. In the NE, this group crops out along Khor Arbaat and Khor Salatib and in the SW along Khor Samadi (Fig. 2). The Arbaat volcanic group at the junction between Khors Arbaat and Salatib (Fig. 2) comprises intercalations of basaltic andesite, rhyolite, intermediate tuff, sandstone, and conglomerate (Fig. 3). The sandstone beds show well-developed channel structures and convolute bedding. Pillow structures were observed in some of the metabasalts. The presence of these pillowed basalts indicate a subaqueous environment of eruption.

The contact between the Arbaat group and the Salatib group is defined by a NE-trending tectonic melange (Fig. 2), about 1 km thick. The melange comprises blocks of Arbaat volcanic rocks up to 8 m across which are enclosed in a sheared carbonate and clastic sedimentary matrix from the Salatib group (Fig. 4).

One suite of five samples from Khor Salatib and another suite of six samples from the Khor Satem area (Fig. 2) were

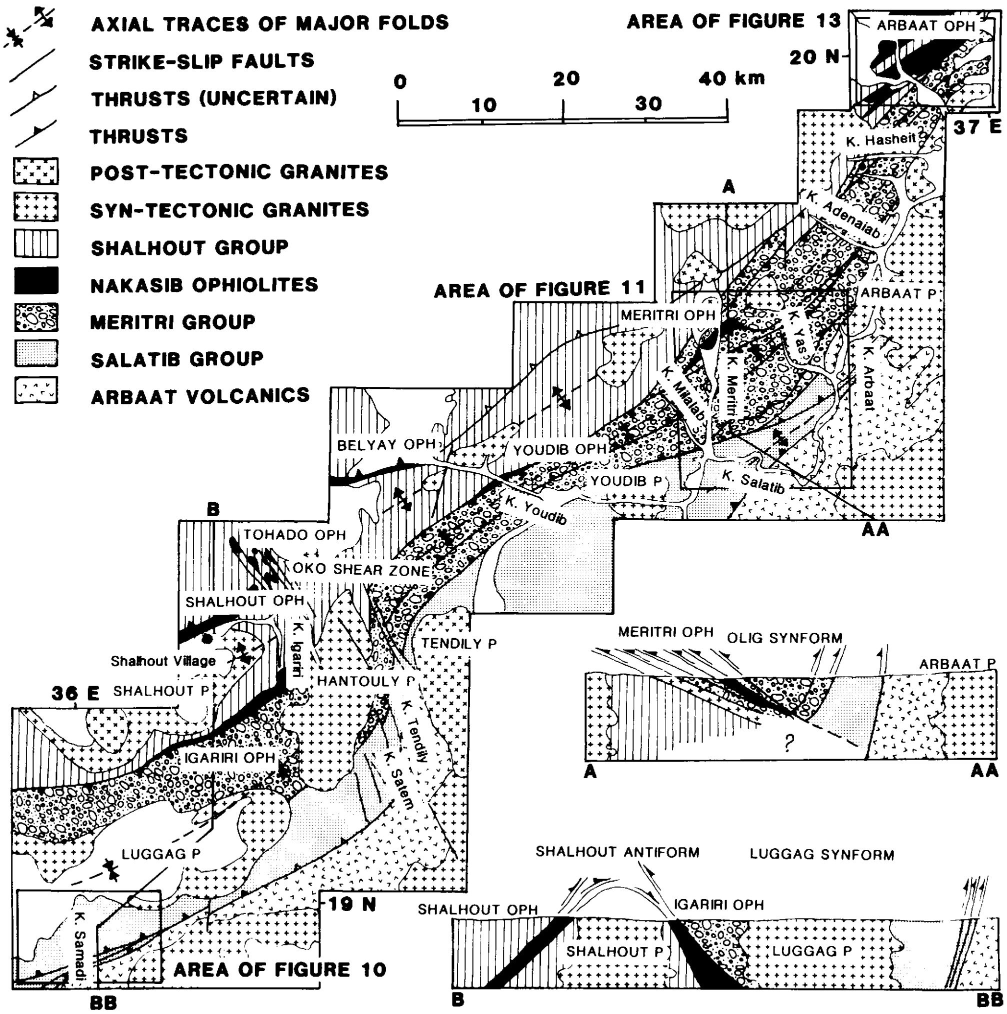

Fig. 2. Geological map of the Nakasib suture. OPH, ophiolite; P, pluton.

collected and analysed for whole rock Rb-Sr age determinations. Methods and standards of analysis follow those outlined by Stern *et al.* (1991). The analytical results are listed in Table 1 and are presented in Fig. 5. Samples from Khor Salatib gave an errorchron age of 722 ± 59 Ma. The samples from Khor Satem gave an errorchron age of 744 ± 137 Ma. When data points from both localities were plotted together an errorchron age of 722 ± 47 Ma is obtained. Initial $^{87}Sr/^{86}Sr$ ratios from both localities are similar and range between 0.70265 and 0.70260 (Fig. 5).

Although the above results are errorchron ages, they indicate the following:

(1) The Arbaat volcanic rocks are pre-accretionary and were formed prior to around 730 Ma ago and not post-tectonic extrusions. They cannot be related to the Asoteriba series or the Awat series as has been suggested (Aye *et al.* 1985). Kabesh (1962) suggested that the Awat volcanic rocks unconformably overlie the older volcano-sedimentary rocks of the Red Sea Hills which were grouped as the Nafardieb series. Klemenic (1985) obtained a whole rock Rb-Sr age of 671 ± 18 Ma from the similar Homogar volcanic rocks in the northern part of the Red Sea Hills. The low initial $^{87}Sr/^{86}Sr$ ratio of the Arbaat volcanic rocks (0.70265–0.70260) compared to the Homogar volcanic rocks (0.7034) further supports the distinction between the two volcanic suites.

(2) The Arbaat volcanic rocks represent a continuous belt extending from the NE part of the Nakasib suture, through its central part at the vicinity of the Oko shear zone and possibly up to the SW part of the suture (Fig. 2). This is indicated by the similar ages and initial $^{87}Sr/^{86}Sr$ ratios of volcanic rocks from Khor Salatib at the NE part of the suture and Khor Satem to the SW (Fig. 5).

The tectonic setting of the Arbaat volcanic rocks, deduced from geochemical data, is of special interest with respect to the early evolution of the Nakasib suture. The results of chemical analysis for 23 samples from them are listed in Table 2. Methods and standards of analysis are outlined in the caption to Fig. 6. Geochemical analyses for 17 other samples obtained by Reischmann (1986) are also considered here. Locations of geochemical data are shown in Fig. 2.

The samples under consideration include 18 basalts, five basaltic andesites, nine andesites, three rhyolites, three trachyandesites, one dacite, and one hawaiite (Fig. 6a). All of the samples analysed preserve original igneous textures. Alteration is slight and includes development of chlorite and epidote after the mafic minerals and limited breakdown of

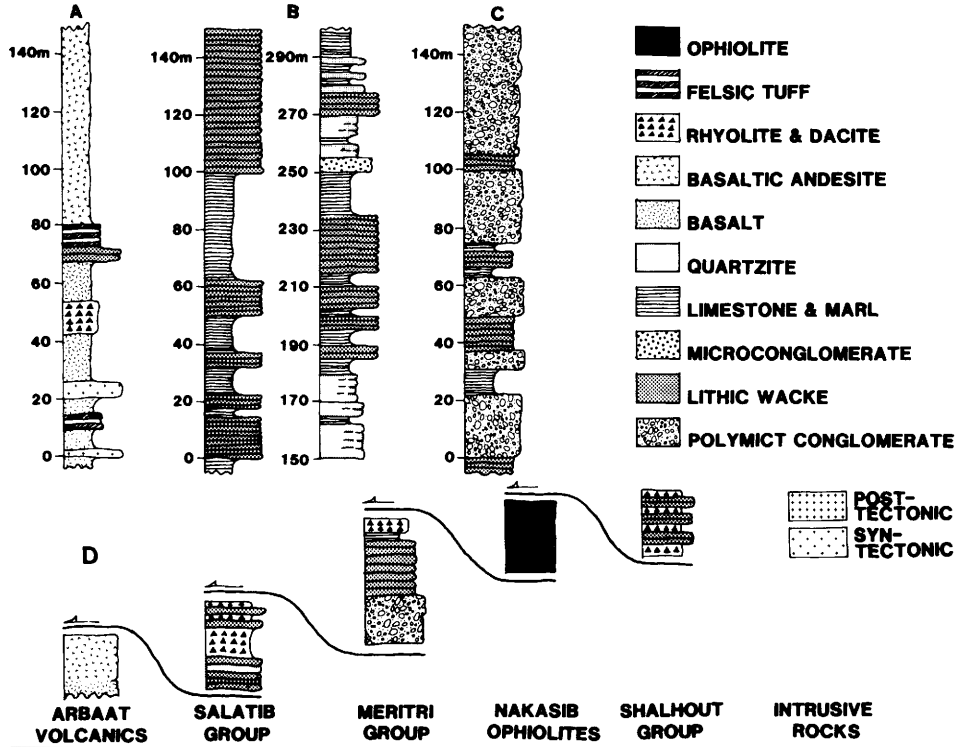

Fig. 3. Stratigraphical chart for rocks of the Nakasib suture. (**A**) Measured section for the lower part of the Arbaat volcanic rocks along Khor Arbaat. (**B**) Representative section for the sedimentary part of the Salatib group along Khor Salatib. (**C**) Representative section for the conglomerate of the Meritri group along Khor Meritri. (**D**) Stacking order observed in the nappes of the Nakasib suture.

Fig. 4. A photograph from the melange zone which separates the Arbaat volcanics from the Salatib group showing a large sigmoidal volcanic fragment enclosed in a sheared carbonate and clastic sedimentary matrix.

Table 1. *Geochronological data of the Arbaat volcanic rocks*

Sample No.	Rb(ppm)	Sr(ppm)	$^{87}Rb/^{86}Sr$	$^{87}Sr/^{86}Sr$
Geochronological data for samples from Khor Arbaat				
H-13-1	6.9	393.0	0.05046	0.70314
H-13-7	46.8	134.0	1.01096	0.71327
H-16-5	10.7	345.0	0.08951	0.70349
H-16-15	2.9	346.0	0.02454	0.70300
H-17-2	18.9	363.0	0.15079	0.70403
Geochronological data for samples from Khor Satem				
29-3b	13.5	515.0	0.07551	0.70355
29-3c	5.1	575.9	0.02534	0.70292
29-3d	10.4	530.4	0.05644	0.70320
29-3e	20.4	472.2	0.12471	0.70292
29-3f	5.4	611.9	0.02555	0.70292
29-3g	2.7	545.7	0.01452	0.70280

Ca-plagioclase into sericite and calcite. All of the samples, with the exception of 6, plot in the tholeiitic field of the $FeO^*/MgO–SiO_2$ diagram (Fig.6b).

Tectonic discriminant diagrams are employed for the Arbaat volcanic rocks (Figs 7 & 8). In the TiO_2–Zr and Zr/Y–Zr diagrams (Pearce 1980); they concentrate in the within-plate field (Fig. 7a and b), and most of them have low Nb concentrations (1.0–10.4 ppm). This is reflected in the concentration of data points in the volcanic arc magma field in the Nb–SiO_2 diagram (Fig. 8; Pearce & Gale 1977). The low Nb concentration (generally regarded as indicating arc setting) of the Arbaat volcanic rocks is not easy to reconcile with a continental rift tectonic setting. Low concentrations of Nb are also observed from rift basalts

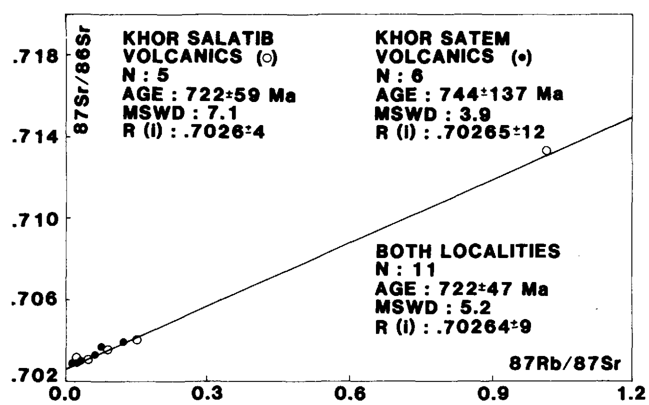

Fig. 5. The geochronology of the Arbaat volcanic rocks. Rb and Sr were analysed by isotopic dilution on the UTD 12″-radius and MAT 261 solid source mass spectrometers. Total processing blank are ≤3 ng Sr and ≤0.1 ng Rb. Age regressions were carried out using the York II treatment of data (York 1969) and all uncertainties are 2 sigma.

Table 2. *Geochemical data of the Arbaat volcanic rocks*

	Khor Salatib																	Khor Satem						Nakasib ophiolites		
Sample	H-13-1	H-13-2	H-13-3	H-13-4	H-13-5	H-13-6	H-13-7	H-13-8	H-13-9	H-13-10	H-16-2	H-16-3	H-16-5	H-16-15	H-17-1	H-17-2	H-17-3	29-3B	29-3C	29-3D	29-3E	29-3F	29-3G	19-2	20-3A	20-3B
Major elements (%)																										
SiO_2	51.60	49.99	57.30	52.93	51.15	49.07	76.50	45.13	48.62	61.57	55.48	49.80	48.96	53.78	49.22	77.75	52.90	59.02	56.26	52.01	61.39	51.71	56.06	49.19	50.05	51.20
TiO_2	0.81	1.82	0.74	1.24	2.93	2.96	0.28	1.66	1.98	0.72	1.94	2.97	3.29	1.75	1.29	0.28	1.47	0.79	1.33	1.18	1.32	1.38	1.33	0.07	0.88	0.87
Al_2O_3	19.02	15.15	18.04	19.52	13.31	13.63	13.61	16.95	16.03	18.80	14.21	13.38	13.97	15.77	18.52	11.20	17.07	18.28	17.38	19.89	16.17	18.16	17.10	18.23	18.21	18.91
Fe_2O_3	8.48	13.06	6.43	9.10	15.00	14.59	1.90	13.78	15.23	4.81	11.94	14.46	14.24	11.13	10.42	3.25	10.45	7.68	9.35	10.22	8.40	11.10	9.34	5.69	9.38	8.36
MgO	6.22	5.90	5.89	4.20	5.16	5.57	0.20	8.69	8.55	2.42	3.95	5.17	5.45	5.14	7.55	0.08	4.96	3.64	5.01	5.06	3.00	4.64	4.75	9.14	8.39	5.39
CaO	10.58	10.38	6.26	7.84	9.38	9.88	1.51	5.90	5.32	5.25	6.79	9.28	8.44	7.64	9.50	0.24	8.18	6.83	7.95	8.02	5.94	9.10	8.48	18.29	10.55	12.65
Na_2O	2.36	2.76	4.71	4.23	2.34	2.35	5.12	4.41	3.21	5.24	3.37	3.33	4.01	3.92	2.50	3.32	3.91	3.54	2.98	3.82	3.53	3.08	2.89	0.50	2.86	2.78
K_2O	0.39	0.36	0.79	0.93	1.42	0.74	2.42	1.80	0.40	0.85	1.39	0.99	0.90	0.21	0.92	4.35	0.79	1.09	0.50	0.78	1.37	0.63	0.30	<0.01	0.10	0.21
P_2O_5	0.15	0.31	0.24	0.24	0.59	0.61	0.07	0.23	0.38	0.28	0.39	0.62	0.73	0.36	0.24	0.05	0.30	0.19	0.45	0.27	0.28	0.29	0.45	<0.01	0.12	0.15
Total	99.61	99.73	100.40	100.23	101.28	99.40	101.61	98.55	99.72	99.94	99.46	100.00	99.99	99.70	100.16	100.52	100.03	101.06	101.21	101.25	101.40	100.09	100.70	101.12	100.54	100.52
Trace elements (ppm)																										
Ni	71	56	38	118	36	44	6	47	33	20	31	42	34	31	106	40	48	18	50	35	50	43	48	91	133	60
Zn	74	81	68	72	122	137	22	92	245	80	118	136	135	102	87	97	95	78	103	88	75	95	102	14	66	70
Cu	124	25	27	85	151	134	12	19	18	65	280	139	54	505	49	55	89	45	79	135	28	79	46	136	32	106
Zr	41	133	103	56	240	247	344	192	176	81	201	259	206	179	96	140	126	127	210	109	376	111	209	<1	61	100
Nb	1.0	3.6	2.7	1.6	8.9	10.2	10.4	5.3	5.1	2.8	5.9	10.1	8.9	5.2	3.1	4.6	4.1	2.4	6.0	2.2	5.9	2.9	6.3	<1	1.2	2.0
Rb	7	5	19	12	18	10	49	20	6	11	23	13	11	3	19	22	13	14	4	10	20	4	2	<1	<1	4
Sr	379	355	418	722	332	389	133	416	232	951	307	347	359	335	378	381	394	511	544	457	437	536	537	616	395	433
Th	<2	<2	<2	<2	<2	<2	7	2	<2	<2	2	2	<2	3	<2	2	<2	2	<2	<2	<2	<2	2	<2	<2	<2
Pb	<2	2	<2	<2	2	2	<2	2	3	<2	<2	3	<2	<2	<2	<2	<2	5	4	2	5	3	5	<2	<2	3
Y	14	35	24	8	52	51	51	38	42	7	45	53	48	38	22	30	28	21	31	21	44	25	31	3	18	20
Cr	177	125	75	233	107	120	2	99	117	27	48	95	56	96	157	112	135									
V	216	363	177	150	360	403	6	225	351	95	321	373	361	271	207	233	229									
Sc	32	56	29	22	45	50	7	36	48	9	43	43	45	39	32	34	37									
Ba	92	145	136	264	334	196	427	220	180	311	368	173	253	188	158	284	196									
La	6	7	9	2	21	22	27	13	15	6	14	22	19	12	11	9	11									
Ce	10	23	11	15	47	45	68	30	32	22	33	44	40	32	16	26	24									
Nd	4	16	11	10	33	36	36	20	26	15	24	37	33	24	12	14	17									

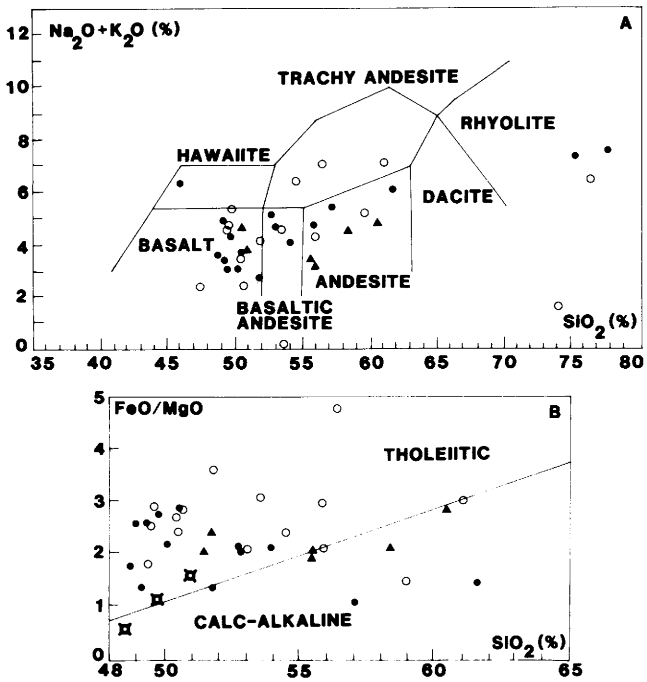

Fig. 6. Plot of major element data from the Arbaat volcanic rocks. The major element analysis of our 23 samples was carried out by XRF at the University of Oklahoma using fused disks. Trace element concentrations were obtained by XRF at the same laboratory using pressed pellets. Procedures of preparation and analysis of samples follow methods outlined in Williams (1972). (**A**) ALK–SiO_2 diagram (Cox *et al.* 1979). (**B**) FeO*/MgO–SiO_2 diagram. Solid circles and triangles represent data acquired by authors from Khor Arbaat area and Khor Satem area respectively. Stars are data points from the basalts of the Nakasib ophiolites. Open circles are data points from Arbaat volcanic rocks from Reischmann (1986)

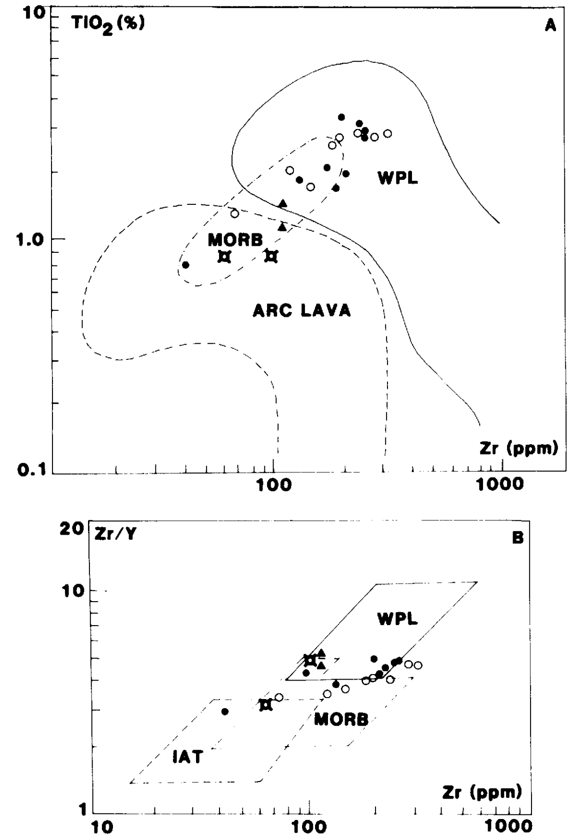

Fig. 7. Tectonic discriminant diagrams for the Arbaat basalts. (**A**) TiO_2–Zr diagram (Pearce 1980). (**B**) Zr/Y–Zr diagram (Pearce 1980). Solid circles and triangles represent data acquired by the authors from Khor Arbaat area and Khor Satem area respectively. Stars are data points from the basalts of the Nakasib ophiolites. Open circles are data points from Arbaat volcanic rocks from Reischmann (1986). WPL, within plate lava; MORB, mid-ocean ridge basalts; IAT, island arc tholeiites.

related to opening of the Atlantic ocean (Froelich & Gottfried 1988; Fodor *et al.* 1985). The Arbaat volcanic rocks show remarkable geochemical similarities to these basalts (Fig. 9a). Moreover, the same geochemical pattern of Nb depletion was observed from some of post-tectonic within-plate Pan-African dykes of south Sinai (Friz-Topfer 1991) and the *c.* 710 Ma old Shadli rift volcanic rocks of the south Eastern Desert of Egypt (Stern *et al.* 1991; Fig. 9b). This low-Nb subductional geochemical signature which appears in some rift tholeiites may indicate that the subcontinental lithosphere through which these basalts erupted preserved the signature of former subduction processes (Thompson *et al.* 1983). The chemical composition of the lithosphere which underlies the Arbaat volcanic rocks is not known. However, it is likely that this lithosphere evolved in the subductional processes which resulted in the formation of the Haya arc terrane (Kroner *et al.* 1987, Kroner *et al.* 1991). As a consequence, the arc signature represented by low Nb concentration may have been inherited by the Arbaat volcanic rocks.

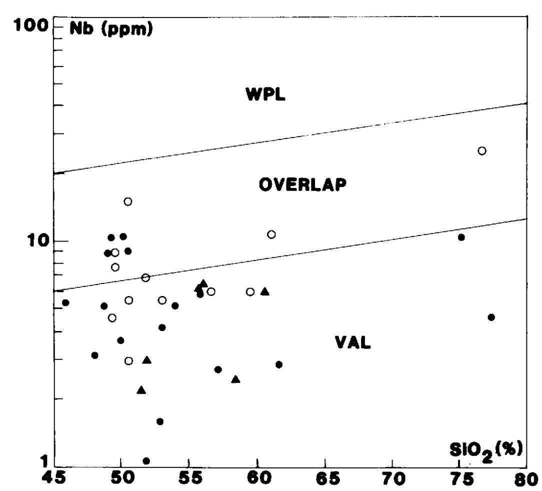

Fig. 8. Nb–SiO_2 diagram (Pearce & Gale 1977) for the Arbaat volcanic rocks. Solid circles and triangles are data acquired by the authors from Khor Arbaat area and Khor Satem area respectively. Open circles are from Reischmann (1986). WPL, within plate lava; VAL, volcanic arc lava.

The Salatib group

This group is made up of intercalated clastic sediments, carbonate, rhyolite and felsic tuff. It is separated by thrusts

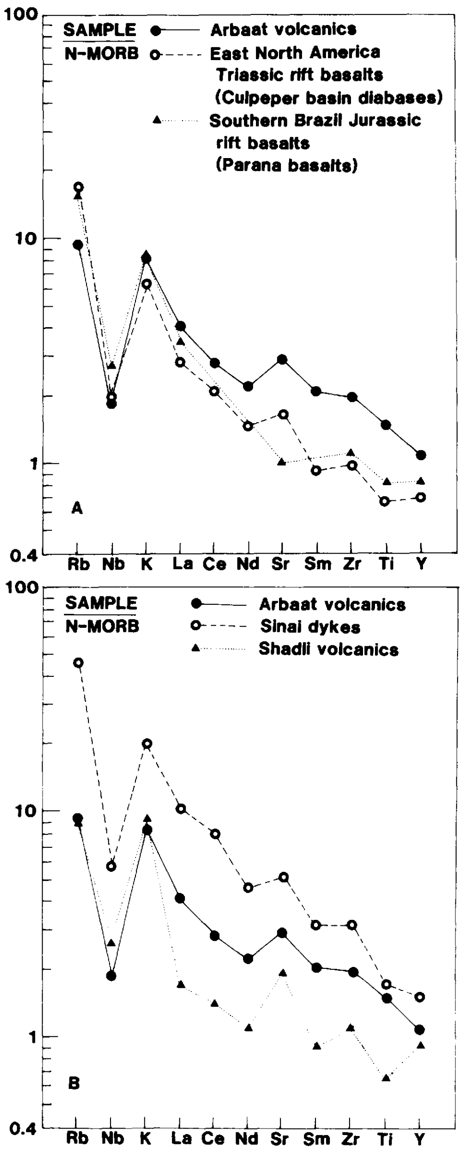

Fig. 9. Normalized element plots comparing the Arbaat basalts with (**A**) basalts related to the opening of the Atlantic ocean; and (**B**) Other rift basalts from the Nubian Shield. Note that all volcanics show depletion in Nb. For the Arbaat volcanic rocks $n = 11$. The Sm data points are from Reischmann (1986). For the Culpeper basin diabases $n = 12$ and Data points are from Froelich & Gottfried (1988). For Parana basalts $n = 7$ and data points are from Fodor *et al.* (1985). For the Sinai dykes $n = 3$ and data points are from Friz–Topfer (1991). For the Shadli basalts $n = 6$ and data points from Stern *et al.* (1991).

from the subjacent Arbaat volcanics and the overlying Meritri group (Fig. 2). The Salatib group is folded into a SE-verging, NE-plunging antiform–synform structure. Fold geometry and primary structures (mainly graded bedding and cross bedding) suggest that the general younging direction of the group is from SW to NE.

In the southwest, the Salatib group occupies a major antiform-synform which is defined here as the Samadi structure (Fig. 10). The 1.2 km thick succession comprises mainly lithic wacke, microconglomerate and intraformational conglomerate intercalated with thin felsic to intermediate tuffs and limestone beds (Fig. 10). In the central part of the Nakasib suture the group comprises intercalations of rhyolite, conglomerate, lithic wacke, mudstone, ignimbrite, felsic volcanics and welded tuff. In the northeast part of the Nakasib suture, the Salatib group occupies the NE-trending Salatib antiform (Fig. 11). The core of this antiform is dominated by lithic wacke with minor intercalations of pebbly lithic wacke and microconglomerate. The limbs of the Salatib antiform are defined by thin and well bedded intercalated microconglomerate, purple sandstone, limestone, rhyolite, quartzite and marl.

The Meritri group

This group is made up of four formations. These are from oldest to youngest: conglomerate; lithic wacke; intercalated limestone, red sandstone and felsic tuff; and felsic volcanic rocks (Fig. 11). These are folded into the NE-trending Olig synform (Fig. 11).

The conglomerate occupies the core of the downward-facing Olig synform (Fig. 11) and is made up of abundant polymict conglomerate intercalated with minor lithic wacke and limestone beds. It shows an apparent thickness of about 4 km along Khor Meritri. Allowing for folding and thrusting, the original thickness in Khor Meritri is *c.* 2 km.

The polymict conglomerate is matrix supported. The matrix consists of lithic wacke and minor carbonate. The clasts comprise granite, granodiorite, diorite, rhyolite, ignimbrite and carbonate as well as a few clastic sedimentary clasts. Intermediate to felsic volcanic clasts dominate the SW extension of the unit, W of the Oko shear zone. In the NE, along Khor Meritri, plutonic clasts are most abundant and form about 50% of total clasts. Volcanic clasts are about 35%. Sedimentary clasts represent about 15%.

The lithic wacke unit occupies the limbs of the Olig synform (Fig. 11) with an original thickness of *c.* 2.5 km. It is made up of lithic wacke intercalated with minor felsic volcanic layers and limestone beds. Locally the lithic wacke grades into microconglomerate with dominant felsic volcanic fragments. Sedimentary structures include graded bedding (Fig. 12a), cross bedding (Fig. 12b), and channels. The channel structure and cross bedding indicate that the palaeocurrent direction was from SE to NW.

The intercalation of limestone, red sandstone, and felsic tuffs outcrops only along Khor Meritri and Khor Milalab (Fig. 11), thinning out along strike. It occupies part of the south limb of the Olig synform where its upper boundary is partially truncated by the thrust which separates the Meritri group from the Salatib group (Fig. 11). The original thickness of the entire unit is estimated to be about 200 m along Khor Meritri.

The upper part of the Meritri group is dominated by felsic volcanic rocks and clastic sediments. These rocks crop out along Khor Yas (Fig. 2) where they occupy an antiform (Fig. 11) and reach a thickness of 600 m. The clastic sediments occupy the stratigraphically lower position and are made up of thin intercalations of conglomerates, sandstones, and minor limestone beds. The volcanic rocks are stratigraphically higher and are made up of tuffaceous volcanics, pyroclastics and rhyolites with well-developed flow banding.

This work provides five points which constrain interpretations of the depositional setting of the Salatib and Meritri groups. (1) The presence of cross bedding and

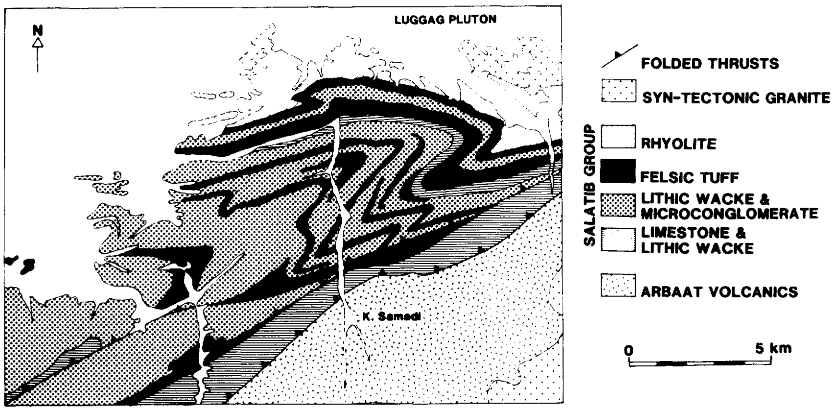

Fig. 10. Geological map of the Samadi area (for location see Fig. 2).

channel structure indicate a subaerial depositional setting of possible proximal fluvial and alluvial fans and plains. (2) The palaeocurrent was from SE to NW as indicated by the cross bedding. (3) The large clast size and poor sorting of the conglomerates suggest a high energy depositional regime and support a possible fluvial depositional setting for the lower part of the Meritri group. (4) On the other hand, the presence of graded bedding suggests a deep water setting of possible submarine fans. (5) The rift tectonic setting of the Arbaat volcanic rocks, together with the above depositional characteristics suggest that the Meritri group was deposited on a steep slope of a rifted block, possibly the northern margin of the Haya terrane.

Rift volcanic rocks are generally followed and accompanied by alluvial fan and/or submarine fans deposits (Crossely 1979). Hence, the Salatib group possibly represents fan deposits accumulated above the Arbaat rift volcanic rocks but it is not yet possible to decide whether the Salatib group represent alluvial fans or submarine fans. The oldest part of the Meritri group shows gross similarities to submarine fans which are characterized by accumulation of clastic sediments under progressively deeper water conditions that accompany opening of incipient ocean basins (Miall 1990). The basal lithofacies of submarine fans is often characterized by development of chaotic deposits of exotic clasts and contorted and disrupted strata (Pickering *et al.* 1986). This is very similar to the polymict conglomerate of the Meritri group. Moreover, the Meritri conglomerates resemble those of Jurassic–Cretaceous fan-deltas to submarine fans which were deposited along scraps in tilted blocks of east Greenland (Surlyk 1984). Along the faulted blocks, fan-deltas and submarine fan conglomerates are followed by dominant deposition of sands of submarine distal fans (Pickering *et al.* 1986; Surlyk 1987), exemplified here by the lithic wackes of the Meritri group. In this way, the Salatib and Meritri groups may represent distal and proximal sedimentary deposits.

The Nakasib ophiolite

This group comprises mafic and ultramafic rocks which, although dismembered, show most of the characteristics of ophiolites. The rocks occur as fragments and lenses in two parallel belts which outline a folded nappe. This folded thrust geometry is defined by the Shalhout antiform in the SW part of the Nakasib suture (Fig. 2). In the N limb of the fold, the thrust plane is defined by a narrow (less than 5 m thick) NW-dipping (45°) talc and serpentinite band. The thrust separates structurally lower dacitic volcanics of the Shalhout group from gabbros and pyroxenites of the

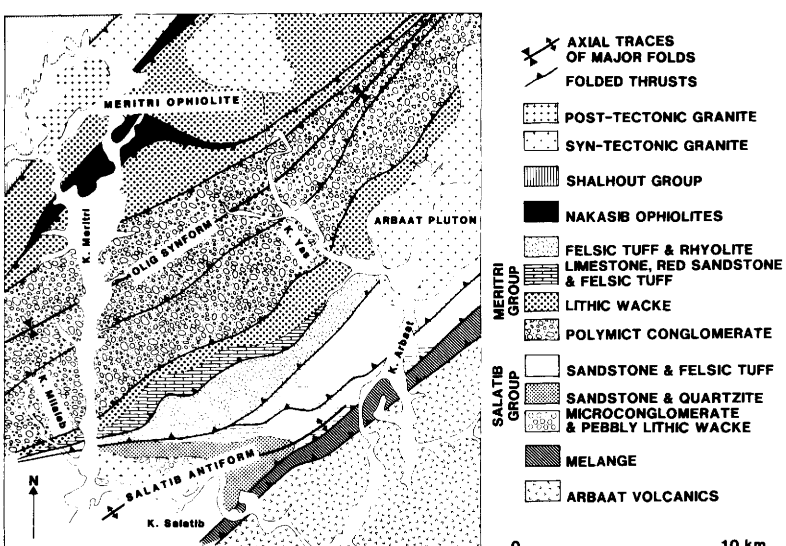

Fig. 11. Geological map of the NE-part of the Nakasib suture (for location see Fig. 2).

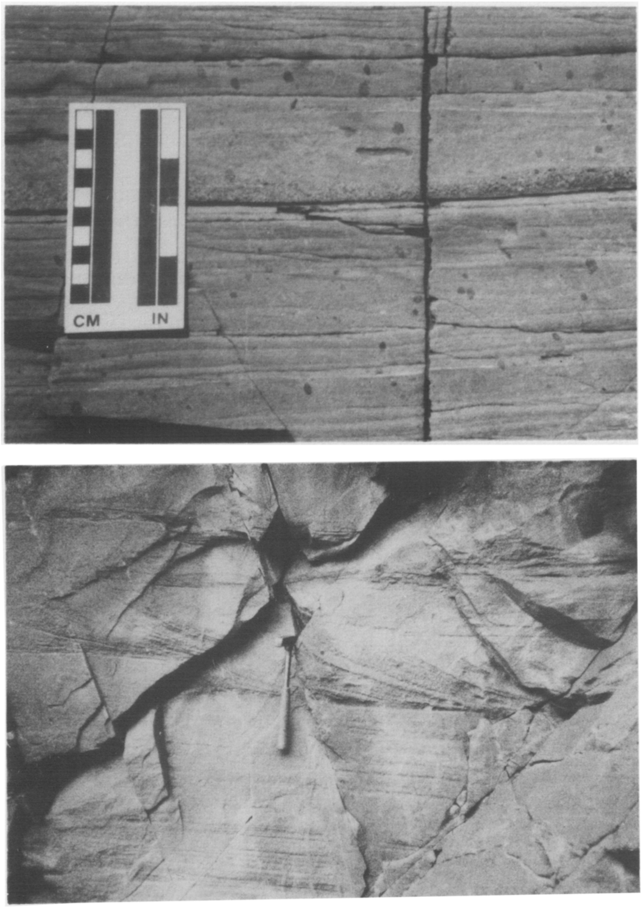

Fig. 12. (**A**) Graded bedding from the lithic wacke of the Meritri group. (**B**) Cross bedding from the lithic wacke of the Meritri group.

ophiolite which occupy the structurally higher position. On the southern limb of the Shalhout antiform, the foliation along the thrust dips steeply to moderately to the SE. In the NE part of the Nakasib suture, a similar SE-dipping thrust plane that is defined by talc schist is recorded from the ophiolite along Khor Meritri.

Six ophiolite occurrences are recorded along the Nakasib suture: Arbaat, Meritri, Balyay, Youdib, Shalhout and Igariri (Fig. 2). A major ophiolite occurrence which is discordant with the general NE-trend of the Nakasib suture occupies the area around Jebel Tohado (Fig. 2). The discordant trend is due to deflection by the Oko shear zone (Fig. 2).

The Arbaat ophiolite (Fig. 13) contains sheared fragments of serpentinite melange, isotropic gabbro, pillowed basalt, jasper and chert. The Meritri ophiolite is composed of talc schist and tectonic melange which contains fragments of ultramafic rocks enclosed in a clastic sedimentary matrix. Other lithologies include pyroxenite, layered gabbro, and basalt. The Belyay ophiolite is mainly ultramafic melange in which partly serpentinized pyroxenite and magnesite blocks are enclosed in a matrix of sheared serpentinite and talc (Fig. 14). The Youdib ophiolite is a large lens of sheared gabbro. The Shalhout ophiolite comprises serpentinite and talc which enclose large lenses of pyroxenite, isotropic gabbro and basalt. These lithologies are intercalated with clastic sedimentary and intermediate volcanic rocks of the Shalhout group. The Igariri ophiolite is made up of sheared serpentinite and gabbro separated by clastic sediments and marble beds.

Limited geochemical data from the pillowed basalts of the Arbaat and Shalhout ophiolites (Fig. 2) suggests that these basalts are tholeiitic (Fig. 6b). These basalts plot in the MORB field of the TiO_2–Zr and Zr/Y–Zr tectonic discriminant diagrams (Fig.7; Pearce 1980).

The Shalhout group

This group occupies the area between the two belts of the Nakasib ophiolites and that to the NW of it (Fig. 2). It was named the Yas volcanic group in the NE-part of the Nakasib suture (Abdelsalam & Stern 1991). We think that the name Shalhout group is more suitable because the group contains clastic sedimentary rocks as well as volcanic rocks, and the group is best exposed around Shalhout village (Fig. 2).

The Shalhout group comprises felsic and intermediate volcanic rocks and fine-grained wackes. Other lithologies include ignimbrite and felsic tuffs. In the NE-part of the Nakasib suture, along Khor Adenaiab, the felsic tuffs of the Shalhout group are in thrust contact with the conglomerates of the Meritri group (Fig. 2). Along Khor Meritri, this thrust contact is decorated by the Meritri ophiolite. Thrust planes in both localities are NW-verging with dips of 7° to 10° along Khor Meritri and 45° to 50° along Khor Adenaiab. Along Khor Adenaiab two distinct units can be observed. The lower unit is made up of fine grained turbidites

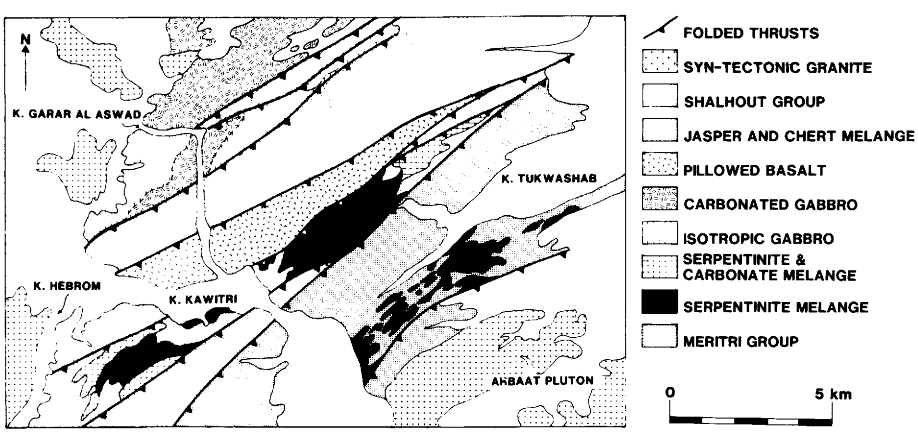

Fig. 13. Geological map of the Arbaat ophiolite (for location see Fig. 2).

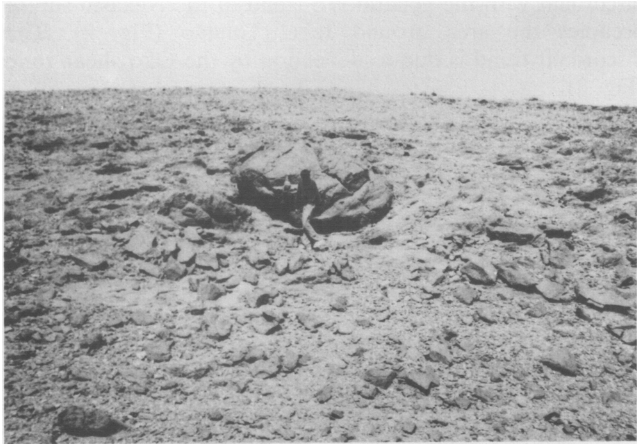

Fig. 14. A large magnesite fragment in a talc and serpentinite matrix from the Belyay ophiolitic melange.

containing graded bedding and cross bedding. The upper unit comprises thin (less than 1 m thick) layers of felsic tuffs and ignimbrite.

Limited geochemical data from the Shalhout volcanic rocks (Abdelsalam & Stern unpublished data) suggest that these rocks are arc-related. This in turn suggests that the Shalhout group may constitute the southernmost extent of the arc volcanic field of the Gebeit terrane (Fitches *et al.* 1983; Vail *et al.* 1984; El Nadi 1984; Klemenic 1985; Klemenic *et al.* 1985; Reischmann 1986).

The intrusive rocks

The stratigraphical groups described above are intruded by various plutonic rocks ranging from gabbro to granite. These can be divided into syn-tectonic and post-tectonic intrusions depending on the presence or absence of planar and linear fabrics. The syn-tectonic intrusions in the SW-part of the suture are mainly granites to adamellites (e.g. the Shalhout pluton and the Luggag pluton (Fig. 2). They occur as small intrusions of about 10 km average diameter. The Shalhout granite occupies the core of the Shalhout antiform whereas the Luggap pluton occupies the core of the Olig-Luggag synform (Fig. 2). Both plutons contain NE- to E-trending upright foliation which corresponds to the axial planar cleavage of the late folds. Moreover, the two plutons show N- to NNW-trending upright foliations and fractures which is parallel to the planar fabric developed during the formation of the Oko shear zone. Almond *et al.* (1989) obtained a whole rock Rb-Sr isochron age of 697 ± 15 Ma from the Shalhout pluton.

The syn-tectonic 'granites' in the NE-part of the Nakasib suture are mainly gabbro to diorite (e.g. the Arbaat pluton and the Youdib pluton; Fig. 2). The Arbaat pluton contains local and faint NE-trending upright foliation. A small dioritic pluton which outcrops at the junction between Khor Meritri and Khor Salatib (Fig. 2) contains NW-dipping foliation and mylonite bands which were developed during the early stage of the Nakasib suture evolution. At the north part of Khor Meritri, north of the Meritri ophiolite, a small, NE-elongated body (less than 2 km wide) of a syn-tectonic granodiorite is stretched parallel to the Meritri ophiolite (Figs 2 and 11). We examined the contact between this body and the Meritri ophiolite and interpreted it as being a thrust for the following reasons: (1) the contact is straight; (2) the dip of the contact is shallow (27°SE); (3) no chilled margin is observed in the pluton; (4) no thermal metamorphic effect is observed in the ophiolite next to the pluton.

The post-tectonic intrusions are mainly granites which are free of any planar fabric related to the Nakasib deformation. One of these granites in the NE part of the Nakasib suture (named the Arbaat pluton by Almond *et al.* 1989) gave a whole rock Rb-Sr isochron age of 552 ± 16 Ma.

DISCUSSION AND CONCLUSIONS

The distinctive lithostratigraphy of the Nakasib suture allows reconstruction of the tectonic setting of this sedimentary–volcanic package. There are two points which constrain the tectonic setting: (1) the geochemistry of the Arbaat volcanic rocks indicates an early extensional tectonic regime consistent with development of a rift basin; and (2) the presence of the Nakasib ophiolites indicates that this rift developed into an ocean basin. Of interest here is whether or not this oceanic basin was accompanied by development of a passive margin.

Miall (1990) outlined three stages for development of a divergent plate boundary: rift; incipient or youthful ocean; and the mature ocean basin stages. Rift development may be characterized by eruption of large volumes of rift basalts as exemplified by the East African Rift (Burke & Kidd 1980). These volcanic rocks are followed by alluvial fan deposition and submarine fans intercalated with rift volcanic rocks (Crossley 1979). This rifting stage of a passive margin development is well preserved along the Nakasib suture in the form of the Arbaat group and possibly the Salatib group where extensive intercalations of clastic sediments and felsic volcanic rocks are present.

The stage of incipient or youthful ocean is characterized by accumulation of clastic sediments under progressively deeper water conditions in the form of submarine fans and other turbidite systems (Miall 1990; Pickering *et al.* 1986). Attempting to identify lithofacies in the Meritri group similar to those of submarine fans is beyond the scope of this work, but units of the lower part of the Meritri group are possible candidates.

During the mature ocean stage, the sequences deposited during the rift and incipient ocean stages are covered by a wedge of carbonate and/or clastic sediments which show evidence of lateral progradation as well as vertical upbuilding. The intercalations of clastic and carbonate sediments of the youngest part of the Meritri group resemble the near-shore/marginal deposits of a mature ocean basin.

The presence of *c.* 730 Ma old Arbaat rift volcanic rocks indicate that the early stage in development of the Nakasib suture was dominated by an extensional tectonic regime which resulted in the formation of an oceanic basin. These rift volcanic rocks, together with possible passive margin deposits, suggest that the Nakasib suture evolved through a complete Wilson cycle orogeny. Figure 15 illustrates the tectonic evolution of the Nakasib suture prior to the late deformational event which resulted in folding of the nappes. This later structural complication will be discussed in Abdelsalam & Stern (in prep.).

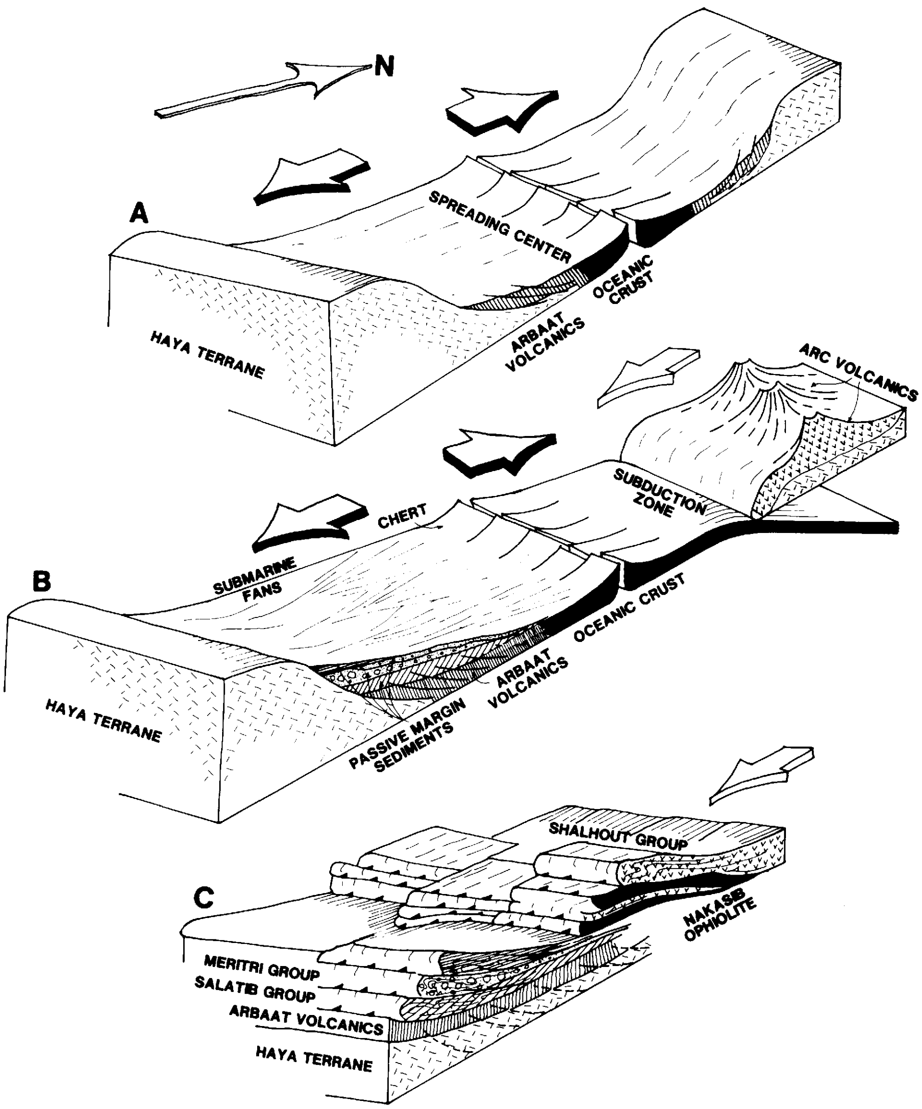

Fig. 15. A three dimensional model illustrating the tectonic evolution of the Nakasib suture. (**A**) Rifting of the Haya terrane and extrusion of the Arbaat volcanics. Development of oceanic crust. (**B**) Development of a passive margin on the southern flank of the oceanic basin. Development of NW-dipping subduction zone on the northern flank of the ocean. Extrusion of arc volcanics above the subduction zone. (**C**) Collapse of the basin and development of SE-verging nappes.

The first field phase (four weeks) of this work was sponsored by the Graduate College of the University of Khartoum. The second field trip (ten weeks) was supported by a grant from NASA to R.J.S.. The TM multi-band and band 5 black and white satellite images were developed in Washington University at St Louis with the help of M. Sultan. The Geological Research Authority of the Sudan provided the authors with the topographic maps, aerial photographs and aerial photomosaics of the area. Major and trace element geochemical data were analyzed for in the University of Oklahoma with the help of B. Weaver. The authors would like to thank K. Nielsen and K. Soegaard for their constructive comments during the preparation of this paper. The authors would also like to thank W. R. Fitches and J. R. Vail for reviewing the manuscript. T. Belo was of great help during the field phase of this work.

References

Abdelsalam, M. G. & Dawoud, A. S. 1991. The Kabus ophiolitic melange, Sudan, and its bearing on the western boundary of the Nubian Shield. *Journal of the Geological Society, London*, **148**, 83–92.

—— & Stern, R. J. 1991. Structural and tectonic evolution of the late Proterozoic Nakasib suture, Red Sea Hills, Sudan. *In:* Rocci, G. & Deschamps, M. (eds) *Recent data in African Earth sciences*, 131–134.

Abdel Rahman, E. M., Harms, U., Schandelmeier, H., Franz, G., Darbyshire, D. P. F., Horn, P. & Muller-Sohnius, D. 1990. A new ophiolite occurrence in NW Sudan—Constraints on late Proterozoic tectonism. *Terra Nova*, **2**, 363–376.

Almond, D. C. 1982. New ideas on the geological history of the basement complex of northeast Sudan. *Sudan Notes and Records*, **59**, 106–136.

—— & Ahmed, F. 1987. Ductile shear zones on northern Red Sea Hills, Sudan and their implication for crustal collision. *Geological Journal*, **22**, 175–184.

——, Darbyshire, D. P. F. & Ahmed, F. 1989. Age limit for major shearing episodes in the Nubian Shield of NE Sudan. *Journal of African Earth Sciences*, **9**, 489–496.

Aye, F., Cheze, Y. & El Hindi, M. A. 1985. Discovery of major massive sulphide province in northeastern Sudan. Symposium on prospecting in desert areas, Rabat, Morocco. *Extended abstracts, Institute of Mining and Metallurgy, London*, 43–48.

Burke, K. & Kidd, W. S. F. 1980. Volcanism on earth through time. *In:* Strangeway, D. W. (ed.) *The continental crust and its mineral deposits*. Geological Association of Canada Special Papers, **20**, 503–522.

Camp, V. E. 1984. Island arcs and their role in the evolution of the western Arabian Shield. *Geological Society of America Bulletin*, **95**, 913–921.

Cox, K. G., Bell, J. D. & Pankhurst, R. J. 1979. *The interpretation of igneous rocks*. Allen and Unwin, London.

Crossley, R. 1979. Structure and volcanism in the S. Kenya Rift. *In: Geodynamic evolution of the Afro-Arabian Rift System*. Accademia Nazionale dei Lincei, Rome, 89–98.

El Nadi, A. H. 1984. *The geology of the late Precambrian metavolcanics, Red Sea Hills, northeast Sudan*. PhD thesis, University of Nottingham.

EMBLETON, J. C. B., HUGHES, D. J., KLEMENIC, P. M., POOLE, S. & VAIL, J. R. 1984. A new approach to the stratigraphy and tectonic evolution of the Red Sea Hills, Sudan. *Bulletin of the Faculty of Earth Sciences, King Abdulaziz University*, **6**, 113–126.

FODER, R. V., CORWIN, C. & ROISENBERG, A. 1985. Petrology of Serra Geral (Parana) continental flood basalts, southern Brazil: crustal contamination, source material, and south Atlantic magmatism. *Contribution to Mineralogy and Petrology*, **91**, 54–65.

FITCHES, W. R., GRAHAM, R. H., HUSSEIN, I. M., RIES, A. C., SHACKLETON, R. M. & PRICE, R. C. 1983. The late Proterozoic ophiolite of Sol Hamed, NE Sudan. *Precambrian Research*, **19**, 385–411.

FRIZ-TOPFER, A. 1991. Geochemical characterization of Pan-African dyke swarms in southern Sinai: from continental margin to intraplate magmatism. *Precambrian Research*, **49**, 281–300.

FROELICH, A. J. & GOTTFRIED, D. 1988. An overview of early Mesozoic intrusive rocks in the Culpeper basin, Virginia and Maryland. *In:* FROEICH, A. J. & ROBINSON, JR., G. R. (eds) *Studies of the early Mesozoic basins of the eastern United States*. US Geological Survey Bulletin. **1776**, 151–164.

KABESH, M. L. 1962. *The geology of the Muhammed Qol sheet*. Memoir of the Geological Survey of the Sudan, **3**.

KLEMENIC, P. M. 1985. New geochronological data on volcanic rocks from northeast Sudan and their implication for crustal evolution. *Precambrian Research*, **30**, 263–276.

—— & POOLE, S. 1988. The geology and geochemistry of upper Proterozoic granitoids from the Red Sea Hills, Sudan. *Journal of the Geological Society, London*, **145**, 635–643.

——, —— & ALI, S. E. M. 1985. The geochemistry of upper Proterozoic volcanic groups in the Red Sea Hills of NE Sudan—evolution of a late Proterozoic volcanic arc system. *Journal of the Geological Society, London*, **142**, 1221–1233.

KRONER, A. 1984. Late Precambrian tectonics and orogeny: A need to redefine the term Pan-African. *In:* KLERKX, J. & MICHOT, J. (eds) *African Geology*. Musee Royal de l'Afrique Central Tervuren, Belgium, 23–28.

—— 1985. Ophiolites and the evolution of tectonic boundaries in the late Proterozoic Arabian–Nubian Shield of northeast Africa and Arabia. *Precambrian Research*, **27**, 277–300.

——, GREILING, R., REISCHMANN, T., HUSSEIN, I. M., STERN, R. J., DURR, S., KRUGER, J. & ZIMMER, M. 1987. Pan-African crustal evolution in northeast Africa. *In:* KRONER, A. (ed.) *Proterozoic lithosphere evolution*. American Geophysical Union, Geodynamic Series, **17**, 235–257.

——, STERN, R. J., LINNEBACKER, P., MANTON, W., REISCHMANN, T. & HUSSEIN, I. M. 1991. Evolution of Pan-African island arc assemblages in the southern Red Sea Hills, Sudan, and in southwestern Arabia as exemplified by geochemistry and geochronology. *Precambrian Research*, **53**, 99–118

MIALL, A. D. 1990. *Principles of sedimentary basin analysis*. Springer-Verlag, New York.

PALLISTER, J. S., STACY. J. S., FISCHER, L. B. & PREMO, W. R. 1988. Precambrian ophiolites of Arabia: Geologic settings, U–Pb geochronology, Pb-isotope characteristics, and implication for crustal accretion. *Precambrian Research*, **38**, 1–54.

PEARCE, J. A. & GALE, G. H. 1977. Identification of ore deposition environment from trace element geochemistry of associated igneous host rocks, *In: Volcanic processes in ore genesis*. Geological Society, London, Special Publication, **7**, 14–24.

—— 1980. Geochemical evidence for the genesis and eruptive setting of lavas from Tethyan ophiolites, *In:* PANAYIOTOU, A. (ed.) *Ophiolites*. Geological Survey Department, Cyprus, 261–272.

PICKERING, K. T., STOW, D. A. V., WATSON, M. P. & HISCOTT, R. N. 1986. Deep-water facies, processes and modes: a review and classification scheme for modern and ancient sediments. *Earth Science Reviews*, **23**, 75–174.

REISCHMANN, T. 1986. *Geologie und genese spatproterozoischer vulkanite der Red Sea Hills, Sudan*. PhD thesis, University of Mainz.

SURLYK, F. 1984. Fan-delta to submarine fan conglomerates of the Volgian–Valanginian Wollaston forland group, east Greenland. *In:* KOSTER, E. H. & STEEL, R. J. (eds) *Sedimentology of gravels and conglomerates*. Canadian Society of Petroleum Geologists Memoir, **10**, 359–382.

—— 1987. Slope and deep shelf gully sandstones, upper Jurassic, east Greenland. *The American Association of Petroleum Geologists Bulletin*, **71**, 464–475.

STERN, R. J., KRONER, A. & RASHWAN, A. A. 1991. A late Precambrian (~710 Ma) high volcanicity rift in the southern Eastern Desert of Egypt. *Geologische Rundschau*, **80**, 155–170.

STOESER, D. B. & CAMP, V. E. 1985. Pan-African microplate accretion of the Arabian Shield. *Geological Society of America Bulletin*, **96**, 817–826.

THOMPSON, R. N., MORRISON, M. A., DICKIN, A. P. & HENDRY, G. L. 1983. Continental flood basalts ... arachnids rule ok? *In:* HAWKESWORTH, C. J. & NORRY, M. J. (eds) *Continental basalts and mantle xenoliths*. Shiva, Nantwich, 158–185.

WILLIAMS, K. 1972. *Introduction to X-ray spectrometry*. Allen and Unwin, London.

VAIL, J. R. 1983. Pan-African crustal accretion in northeast Africa. *Journal of African Earth Sciences*, **1**, 285–294.

—— 1985. Pan-African (late Precambrian) tectonic terranes and the reconstruction of the Arabian–Nubian Shield. *Geology*, **13**, 839–842.

——, ALMOND, D. C., HUGHES, D. J., KLEMENIC, P. M., POOLE., S., NOUR, S. E. M. & EMBLETON, J. C. B. 1984. *Geology of the Wadi Oko-Khor Hayet area, Red Sea Hills, Sudan*. Bulletin of the Geological Research Authority of the Sudan, 34.

YORK, D. 1969. Least squares fitting of a straight line with correlated errors. *Earth and Planetary Science Letters*, **5**, 320–324.

Received 28 November 1991; revised typescript accepted 19 July 1992.